

Phase transition and charge transport through a triple dot device beyond the Kondo regime

Yong-Chen Xiong(熊永臣), Zhan-Wu Zhu(朱占武), Ze-Dong He(贺泽东)

Citation: Chin. Phys. B . 2018, 27(10): 108503. **doi:** 10.1088/1674-1056/27/10/108503

Journal homepage: http://cpb.iphy.ac.cn; http://iopscience.iop.org/cpb

What follows is a list of articles you may be interested in

Effects of edge hydrogenation and Si doping on spin-dependent electronic transport properties of armchair boron-phosphorous nanoribbons

Hong Zhao(赵虹), Dan-Dan Peng(彭丹丹), Jun He(何军), Xin-Mei Li(李新梅), Meng-Qiu Long(龙孟秋)
Chin. Phys. B . 2018, 27(10): 108504. **doi:** 10.1088/1674-1056/27/10/108504

A phenomenological memristor model for synaptic memory and learning behaviors

Nan Shao(邵楠), Sheng-Bing Zhang(张盛兵), Shu-Yuan Shao(邵舒渊)
Chin. Phys. B . 2017, 26(11): 118501. **doi:** 10.1088/1674-1056/26/11/118501

An improved memristor model for brain-inspired computing

Errui Zhou(周二瑞), Liang Fang(方粮), Rulin Liu(刘汝霖), Zhenseng Tang(汤振森)
Chin. Phys. B . 2017, 26(11): 118502. **doi:** 10.1088/1674-1056/26/11/118502

Quantum oscillations and nontrivial transport in $(Bi_{0.92}In_{0.08})_2Se_3$

Minhao Zhang(张敏昊), Yan Li(李焱), Fengqi Song(宋凤麒), Xuefeng Wang(王学锋), Rong Zhang(张荣)
Chin. Phys. B . 2017, 26(12): 127305. **doi:** 10.1088/1674-1056/26/12/127305

Quantum spin Hall and quantum valley Hall effects in trilayer graphene and their topological structures

Majeed Ur Rehman, A A Abid
Chin. Phys. B . 2017, 26(12): 127304. **doi:** 10.1088/1674-1056/26/12/127304

Phase transition and charge transport through a triple dot device beyond the Kondo regime*

Yong-Chen Xiong(熊永臣)†, Zhan-Wu Zhu(朱占武), and Ze-Dong He(贺泽东)

School of Science, and Advanced Functional Material and Photoelectric Technology Research Institution, Hubei University of Automotive Technology, Shiyan 442002, *China*

(Received 7 June 2018; revised manuscript received 3 July 2018; published online 10 September 2018)

Semiconductor quantum dot structure provides a promising basis for quantum information processing, within which to reveal the quantum phase and charge transport is one of the most important issues. In this paper, by means of the numerical renormalization group technique, we study the quantum phase transition and the charge transport for a parallel triple dot device in the strongly correlated limit, focusing on the effect of inter-dot hopping t beyond the Kondo regime. We find the quantum behaviors depend closely on the initial electron number on the dots, and the present model may map to single, double, and side-coupled impurity models in different parameter spaces. An orbital spin-1/2 Kondo effect between the conduction leads and the bonding orbital, and several magnetic-frustration phases are demonstrated when t is adjusted to different regimes. To understand these phenomena, a canonical transformation of the energy levels is given, and important physical quantities with respect to increasing t and necessary theoretical discussions are shown.

Keywords: semiconductor quantum dot device, parallel triple dot structure, quantum phase transition, charge transport, strongly correlated effect

PACS: 85.35.–p, 73.63.–b, 71.27.+a, 73.21.–b **DOI:** 10.1088/1674-1056/27/10/108503

1. Introduction

Semiconductor quantum dot system is considered as a promising candidate for quantum computation due to its ability to confine single electron at discrete energy levels and fine manipulation of parameter space.[1,2] During the past two decades, tremendous progress has been made in understanding the charge and spin transport for single and double quantum dot structures both in experimental and theoretical aspects.[3–9] Recently, the research interest has focused on the triple quantum dot (TQD) systems. Experimentally, TQDs are used to realize multielectron hybrid qubit,[10–13] spectral absorbers,[14,15] charge detectors,[16] and current rectifiers.[17,18] While in the theoretical field, TQD structure offers the potential to study some new fascinating phenomena at low temperatures, including the Kondo effect,[19–22] the Fermi liquid theory,[23,24] the quantum interference,[25,26] and various kinds of quantum phase transitions (QPT).[27–31]

TQD structure could be organized in serial,[32,33] parallel,[34–36] or triangular[37–40] spatial configuration, which may naturally result in different quantum behaviors. Among these configurations, the parallel TQD (PTQD) system is a basic one, which has also inspired a wealth of research. Although many works have been done related to the PTQD model, the charge transport and phase transition are less studied beyond the Kondo regime, which, in all cases, are important for the dynamic and static properties, even for the potential application in nanodevices. In this paper, we consider a PTQD device connected to two conduction leads (see Fig. 1(a)) deviated from the Kondo regime. With the usage of Wilson's numerical renormalization group (NRG) method, we find the inter-dot hopping t may lead to some interesting quantum behaviors in the QPT and charge transport at the strongly correlated limit, quite different from the Kondo regime. More importantly, these behaviors depend closely on the initial electron number on the dots, which is usually adjusted by an external gate voltage. For instance, when the initial charge number of the dots $N_{\rm tot} \approx 0.0$, the linear conductance G reveals a peak shape as t increases. An orbital spin-1/2 Kondo effect could be found between the conduction leads and the bonding orbital. When t is large enough, dot 1 (3) and dot 2 form a spin singlet, while dot 3 (1) is empty. In the regime $N_{\rm tot} \approx 1.0$, G could be considered as a part of the above case and the quantum state is similar to the empty case as t is large enough. When the initial charge number $N_{\rm tot} \approx 2.0$, we find the ground state is a magnetic-frustration phase and G is nearly zero when t is absent. This phase is sensitive to t, and is replaced by another mixture state even t is just 0.1×10^4. A first order QPT could be identified both in dynamic and static physical quantities.

We organize the remaining sections as follows. In Section 2, we present the model Hamiltonian, and the calculation formulas. In Section 3, we describe the numerical result and

*Project supported by the National Natural Science Foundation of China (Grant No. 11504102), the Scientific Research Items Foundation of Hubei Educational Committee (Grant Nos. Q20161803 and D20171803), the Doctoral Scientific Research Foundation of Hubei University of Automotive Technology (Grant No. BK201407).

†Corresponding author. E-mail: xiongyc_lx@huat.edu.cn

© 2018 Chinese Physical Society and IOP Publishing Ltd

discussion. Finally, a conclusion is given in Section 4.

2. Model, method, and formulas

The schematic view of the PTQD structure connected to two conduction leads (source (S) and drain (D)) is presented in Fig. 1(a), and the second quantized Hamiltonian for the whole system is written as

$$H = H_{\rm S} + H_{\rm D} + H_{\rm dots} + H_{\rm T}. \tag{1}$$

Here, $H_{\rm S}$ and $H_{\rm D}$ correspond to the noninteracting source and drain leads respectively with H_α ($\alpha =$ S, D): $H_\alpha = \sum_{k\sigma}\epsilon_{\alpha k}c^\dagger_{\alpha k\sigma}c_{\alpha k\sigma}$, where $c^\dagger_{\alpha k\sigma}$ ($c_{\alpha k\sigma}$) is the creation (annihilation) operator for an electron with wave vector k, spin σ ($\sigma =\uparrow$ or $\downarrow$) in lead α, and $\epsilon_{\alpha k}$ denotes the single-electron energy. $H_{\rm dots}$ describes the energy of the PTQD:

$$H_{\rm dots} = \sum_{i=1,\sigma}^{3}\epsilon d^\dagger_{i\sigma}d_{i\sigma} + \sum_{i=1}^{3}U n_{i\uparrow}n_{i\downarrow} - \sum_{i<j}t_{ij}(d^\dagger_{i\sigma}d_{j\sigma} + {\rm H.c.}). \tag{2}$$

Here, $d_{i\sigma}$ ($d^\dagger_{i\sigma}$) is the annihilation (creation) operator for the electrons on dot site i ($i = 1,2,3$). $n_{i\sigma} = d^\dagger_{i\sigma}d_{i\sigma}$ is the number operator. ϵ and U are the energy level and the intra-orbital Coulomb repulsion respectively, while t_{ij} describes the inter-dot hopping between dots i and j. To avoid too many parameters, we choose $t_{ij} = t$. Finally, the last term in Eq. (1) illustrates the tunneling coupling between conduction bands and dot levels: $H_T = \sum_{\alpha ki\sigma}(\tau_{\alpha ki\sigma}c^\dagger_{\alpha k\sigma}d_{i\sigma} + {\rm H.c.})$. Here, $\tau_{\alpha ki\sigma}$ describe the couplings of the k,σ electron states belonging to lead α to the i-th dot site. We assume $\tau_{\alpha ki\sigma}$ is symmetric with respect to the source and drain leads.

In the present work, we are mainly interested in the QPT and the charge transport of the PTQD device in the strong correlation regime, thus a sophisticated many-body technique must be used. Therefore, we use the NRG method,[41–43] to solve Eq. (1), which is an ideal technique to calculate both static and dynamical properties of the Anderson-type model. We first choose a constant density of states for the conduction leads $\rho_0 = 1/(2D)$, with $2D$ being the band width, and D is chosen as the energy unit in the following discussions. We also approximate a constant hybridization strength between the conduction band and quantum dots $\Gamma = 2\pi\rho_0|\tau_{\alpha ki\sigma}|^2$. In our NRG calculation, Λ, the renormalization parameter, is set to be $1.8 \sim 2.4$, and the number of the low-lying energy states kept at each iteration is about 3000.

The linear conductance through the PTQD G is calculated by the Meir–Wingreen's formula[44]

$$G = \frac{{\rm e}^2}{h}\int {\rm d}\omega \left[\frac{\partial f(\omega)}{\partial\omega}\right] T(\omega), \tag{3}$$

where $f(\omega)$ is the Fermi function, and $T(\omega)$ is the transmission coefficient, which is defined as

$$T(\omega) = -\frac{1}{2}\Gamma\sum_{ij\sigma}{\rm Im}G_{ij\sigma}(\omega). \tag{4}$$

Here, $G_{ij\sigma}(\omega)$ is related to the retarded dot Green's function $G_{ij\sigma}(t) = -{\rm i}\theta(t)\langle\{d_{i\sigma}(t), d^+_{j\sigma}\}\rangle$, and the Fermi function is chosen as $\epsilon_{k_{\rm f}} = 0$, hence the linear conductance at zero temperature in the limit of zero bias can be written as

$$G = T(\omega = 0)\,{\rm e}^2/h. \tag{5}$$

The spin–spin correlation between dots i and j is labeled as $\langle S_iS_j\rangle$, which could be calculated as follows in the NRG steps:

$$\langle S_iS_j\rangle = \langle S_i^+S_j^-/2 + S_i^-S_j^+/2 + (n_{i\uparrow} - n_{i\downarrow})(n_{j\uparrow} - n_{j\downarrow})/4\rangle, \tag{6}$$

with $S_i^+ = d^\dagger_{i\uparrow}d_{i\downarrow}$ and $S_i^- = d^\dagger_{i\downarrow}d_{i\uparrow}$.

3. Results and discussions

In the following discussion, we fix $\Gamma = 0.01$ and $U = 0.1$. Since $U \gg \Gamma$, the electron–electron interaction on the PTQD becomes significantly important, and the system is in the strong correlation limit. When ϵ sweeps downwards, the total electron number on the dots $N_{\rm tot} = \sum_{i=1}^3\langle n_i\rangle$ increases from empty to full, i.e., $N_{\rm tot} = 0.0$ to 6.0. In the regime of $N_{\rm tot} \approx 3.0$, three dots are singly occupied due to strong U, and a spin$-3/2$ Kondo effect could be found, resulting from the process of a local spin magnitude $1/2$ is screened by the conduction leads. Thus this regime is considered as the Kondo regime,[45] which has inspired a wealth of research in the past decade. Since the effect of the inter-dot hopping t in this regime is referred by some previous works,[27] here we focus our attention on the QPT and charge transport affected by t deviate the Kondo regime.

3.1. Effect of t in the empty regime

Let us start our discussion when the quantum dot energy level ϵ is set to be in the unoccupied regime with $N_{\rm tot} \approx 0.0$. In Figs. 1(b)–1(c), we show the electron number $\langle n_i\rangle$ on each dot, and the spin–spin correlation $\langle S_iS_j\rangle$ between dots i and j at zero temperature as functions of t with fixed $\epsilon = 0.1$. Here, $\langle n_1\rangle = \langle n_3\rangle$ and $\langle S_1S_2\rangle = \langle S_2S_3\rangle$ when t sweeps, since dots 1 and 3 are identical. When $t = 0$, one may see $\langle n_i\rangle \approx 0.0$ and $\langle S_iS_j\rangle \approx 0.0$, since the PTQD is in the frozen-impurity fixed point with no residual spin. With increasing t, the charge number on each dot grows continuously, and $\langle S_iS_j\rangle$ decreases to negative. Because a negative t term in Eq. (2) reduces the total energy of the system, and favors an antiferromagnetic spin arrangement between neighboring dots with an effective strength $J_{\rm AFM} = -4t^2/U$. When t is large enough, $\langle n_1\rangle \approx 0.5$, and $\langle n_2\rangle \approx 1.0$, illustrating that dot 2 is occupied by a single electron, whereas only one of dots 1 and 3 is singly occupied,

and the other one is empty. In this case, $\langle S_1 S_2 \rangle$ reaches to about -0.2, showing a spin singlet between dots 1 (3) and 2 is generated. Therefore, the many-body state of $(n_1 n_2 n_3)$ mainly includes configurations $(\uparrow\downarrow 0)$ (or $(\downarrow\uparrow 0)$) and $(0\uparrow\downarrow)$ (or $(0\downarrow\uparrow)$), where dot 3 (1) is empty, while dots 1 (3) and 2 are singly occupied with antiparallel spin ordering. Here, it is notable that $\langle S_1 S_2 \rangle$ could not reach -0.75 of the ideal spin singlet, because the expected value of n_1 is unequal to 1.0. Besides, one also finds $\langle S_1 S_3 \rangle$ reaches to a larger negative value of -0.1, which can be attributed to the fact that in this regime, the Ruderman–Kittel–Kasuya–Yosida (RKKY) interactions mediated by both the Kondo coupling between the leads and the dots and the inter-dot hopping t, which favor singly occupied states and parallel spin arrangement between different dots, become invalid. Therefore, in order to avoid the intra-orbital Coulomb repulsion and reduce the total energy, there are still some possibilities of dots 1 and 3 to form a negative spin–spin correlation. This behavior is similar to the case where the energy level goes through the intermediate valence regime in multi-quantum dot systems.[45–48]

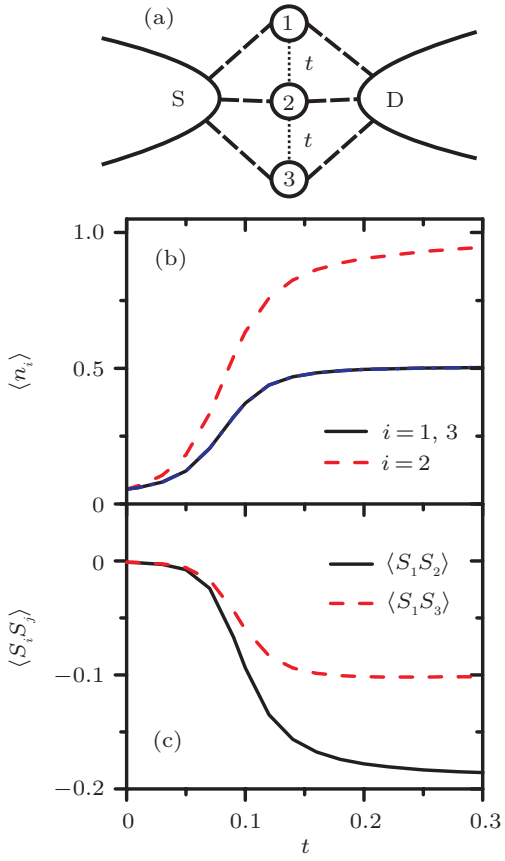


Fig. 1. (color online) (a)Schematic view of the parallel triple dot device connected to source (S) and drain (D) leads. t denotes the inter-dot hopping. (b) Charge occupation on each dot $\langle n_i \rangle$, and (c) Spin correlation $\langle S_i S_j \rangle$ between dots i and j $(i, j = 1, 2, 3)$ at zero temperature as functions of t for fixed energy level $\epsilon = 0.1$. Here, $\langle n_1 \rangle = \langle n_3 \rangle$, $\langle S_1 S_2 \rangle = \langle S_2 S_3 \rangle$ for dots 1 and 3 are identical for symmetry. The remaining parameters are given by $U = 0.1$ and $\Gamma = 0.01$.

Now we study the charge transport through the PTQD. In Fig. 2(a), we depict the transmission coefficient $T(\omega) = T_\uparrow(\omega) + T_\downarrow(\omega)$ at zero temperature in terms of different t. When $t = 0$, $T(\omega) \approx 0.0$, suggesting zero conductance (see Fig. 2(b)). The spectral weight of $T(\omega)$ locates in the regime $\omega > 0$, and a large peak is found at energy $\omega \approx \epsilon$, which corresponds to the process of adding an electron on the bonding orbital as discussed in the following. With increasing t, the spectral weight moves to the direction $\omega < 0$. In this process, the conductance $G = T(\omega = 0)$ increases and reaches to its unitary limit of 1.0 at about $t = 0.075$. When t is large enough, the spectral weight locates in $\omega < 0$ (e.g., $t = 0.016$ in Fig. 3(a)), and the conductance G decreases to 0.0 gradually. In this case, the PTQD is in a local moment formation, and the conductance is suppressed by the spin singlet between dots 1 (3) and 2, similar to the double quantum dot system with strong t in the Kondo regime.[49,50]

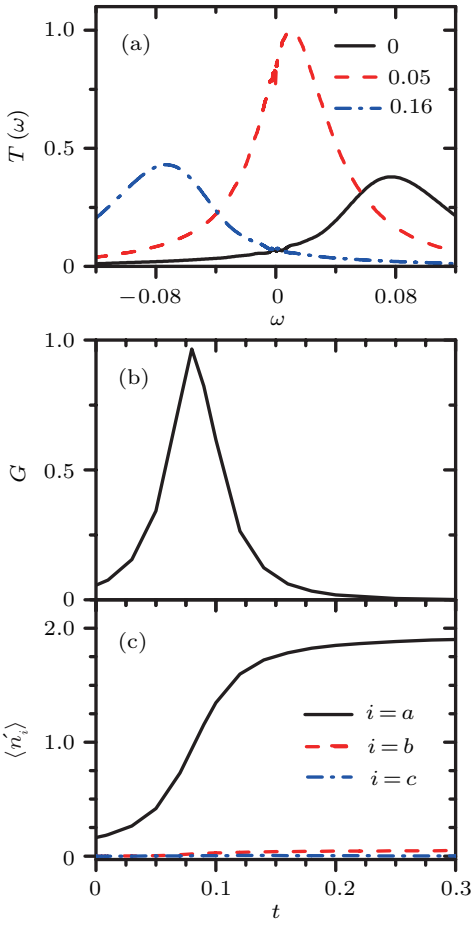


Fig. 2. (color online) (a) Transmission coefficient $T(\omega)$ at zero temperature in terms of different t. (b) Linear conductance G, and (c) charge density on the transformed orbitals $\langle n_i' \rangle$ $(i = a, b, c)$ as functions of t for $\epsilon = 0.1$. The remaining parameters the same as in Fig. 1.

In order to get a clear understanding of the quantum behaviors above, we invite a canonical transformation of the three dot levels:

$$\begin{aligned} f_{a\sigma} &= (d_{1\sigma} + d_{2\sigma} + d_{3\sigma})/\sqrt{3}, \\ f_{b\sigma} &= (d_{1\sigma} - d_{3\sigma})/\sqrt{2}, \\ f_{c\sigma} &= (d_{1\sigma} - 2d_{2\sigma} + d_{3\sigma})/\sqrt{6}. \end{aligned} \tag{7}$$

Under this transformation, the orbital levels are given by $\epsilon_a = \epsilon - 4t/3$, $\epsilon_b = \epsilon + 4t/3$, and $\epsilon_c = \epsilon$, respectively, thus $f_{a\sigma}$ is the bonding orbital, while $f_{b\sigma}$ and $f_{c\sigma}$ are the anti-bonding orbitals. Besides, the H_T item turns out to be $\sqrt{3}\sum_{k\sigma}(\tau_{\alpha k i\sigma} c^{\dagger}_{k\sigma} f_{a\sigma} + \text{H.c.})$, suggesting that only the bonding orbital hybridizes with the conduction leads. In Fig. 2(c), we show the electron number on the bonding and anti-bonding orbitals $\langle n'_i\rangle$ $(i = a,b,c)$ at zero temperature as functions of t. Here, $n'_{i\sigma} = f^{\dagger}_{i\sigma} f_{i\sigma}$. One may see as t increases, $\langle n'_b\rangle$ and $\langle n'_c\rangle$ keep at 0.0, while $\langle n'_a\rangle$ increases gradually, since ϵ_a decreases with increasing t, while ϵ_b (ϵ_c) grows larger (retains at ϵ). Correspondingly, the peak in $T(\omega)$ moves toward the left, for $T(\omega)$ is merely decided by the local density states of the bonding orbital. When $t = 0.075$, $\langle n'_a\rangle \approx 1.0$, and the present model maps to a single impurity Anderson model. An orbital spin-1/2 Kondo effect could be found between the conduction leads and the bonding orbital, and the linear conductance G reaches to its unitary limit (Fig. 2(b)). Here, the value of t could be estimated as follows: when the bonding orbital is singly occupied, annihilating (creating) an electron on this orbital will cost energy $\epsilon - 4t/3$, which gives $t = 0.075$, and is consistent with our NRG result. When t is large enough, the bonding orbital is almost fully occupied, thus the electrons could not transmit the PTQD.

3.2. Effect of t in the singly occupied regime

Now we turn to the case when the PTQD is singly occupied with $N_{\text{tot}} \approx 1.0$. Figures 3(a)–3(b) show $\langle n_i\rangle$, and $\langle S_i S_j\rangle$ as functions of t at zero temperature for fixed $\epsilon = -0.004$. It is seen $\langle n_i\rangle \approx 0.32$ and $\langle S_i S_j\rangle \approx -0.05$ when $t = 0$, indicating the many-body state of $(n_1 n_2 n_3)$ mainly includes configurations such as $(1\,0\,0)$, $(0\,1\,0)$, and $(0\,0\,1)$, where one of the dots is singly occupied while the other two are empty. With increasing t, $\langle n_i\rangle$ grows, while $\langle S_i S_j\rangle$ decreases continuously. When t is large enough, $\langle n_2\rangle \sim 1.0$, while $\langle n_1\rangle \sim 0.5$, similar to the case of $\epsilon = 0.1$ with large t. Thus dot 1 (3) is empty, while dots 3 (1) and 2 are singly occupied with antiparallel spin ordering.

To understand the charge transport through the PTQD, we illustrate $T(\omega)$ for various t, G, and $\langle n'_i\rangle$ as functions of t in Figs. 4(a)–4(c), respectively. One finds $G = T(\omega = 0)$ reaches to almost 1.0 of the unitary limit when t is absent. Because in this case, the charge number on the bonding orbital $\langle n'_a\rangle \approx 1.0$ (Fig. 4(c)), and the orbital spin-1/2 Kondo effect could be found between the conduction leads and the bonding orbital. As t increases, the peak in $T(\omega)$ moves toward the left and the conductance decreases to 0.0 gradually due to decreasing ϵ_a. In this process, $\langle n'_a\rangle$ grows correspondingly, then stabilizes at 2.0 when t is large enough. In Fig. 3(c), we also give $\langle S_i S_j\rangle$ as functions of t for $\epsilon = -0.002$. It is seen the behaviors are similar to the case of $\epsilon = -0.004$, illustrating the discussions above are robust for the regime $N_{\text{tot}} \approx 1.0$.

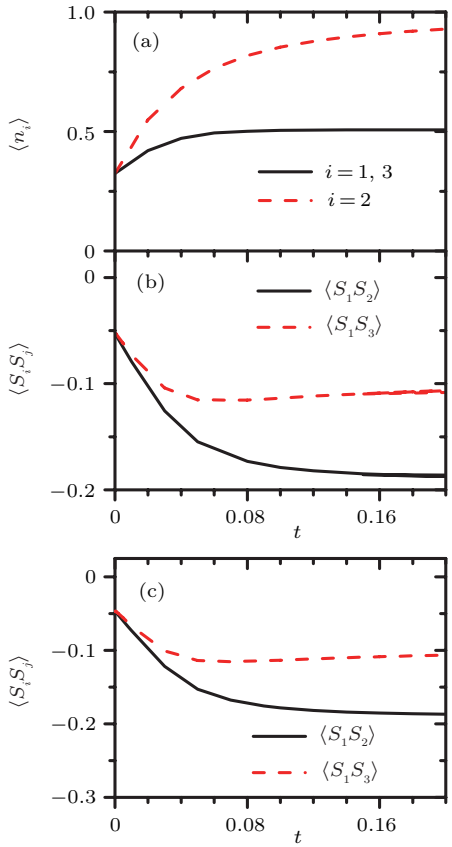


Fig. 3. (color online) (a) and (b) $\langle n_i\rangle$ and $\langle S_i S_j\rangle$ as functions of t for $\epsilon = -0.004$. (c) $\langle S_i S_j\rangle$ as a function of t for $\epsilon = -0.002$. The remaining parameters are the same as in Fig. 1.

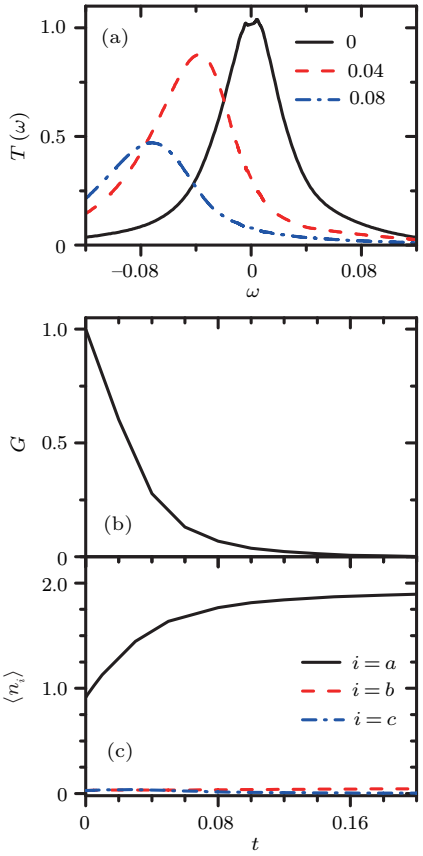


Fig. 4. (color online) (a) $T(\omega)$ at zero temperature in terms of different t. (b) and (c) G and $\langle n'_i\rangle$ as functions of t for $\epsilon = -0.004$. The remaining parameters are the same as in Fig. 3.

3.3. Effect of t in the doubly occupied regime

In this subsection, we focus on the situation where the PTQD is doubly occupied with initial charge numer $N_{\rm tot} \approx 2.0$. In Figs. 5(a)–5(b), we show $\langle n_i \rangle$ and $\langle S_i S_j \rangle$ as functions of t with $\epsilon = -0.01$. When $t = 0$, our NRG results show $\langle n_i \rangle \approx 0.74$ and $\langle S_1 S_2 \rangle \approx -0.10$, thus two of the dots are singly occupied, while the remaining one is nearly empty. The ground state of the system is considered as a magnetic-frustration phase,[45,48] and the antiferromagnetic spin–spin correlation is resulted from the following fact: comparing with the Kondo regime where $N_{\rm tot} \approx 3.0$, the possibilities of each dot being singly occupied is weakened in the regime $N_{\rm tot} \approx 2.0$. This tendency may result in a reduction of the RKKY interaction, which is mediated by the Kondo coupling between conduction leads and quantum dots and favors parallel spin alignment between different dots. Therefore, to reduce the total energy, the local spins are more likely to form an anti-parallel spin ordering on two singly occupied dots. However, this magnetic-frustration phase is sensitive to the inter-dot coupling t, which breaks the symmetry of the three dots. As shown in Figs. 5(a) and 5(b), even t is just 0.1×10^4, $\langle n_1 \rangle$, and $\langle n_2 \rangle$ become different with $\langle n_1 \rangle \approx 0.80$ and $\langle n_2 \rangle \approx 0.60$, accompanied with $\langle S_1 S_2 \rangle \approx -0.20$. Hence the electrons on dots 1 (3) and 2 are arranged anti-ferromagnetically. Besides, one notices $\langle S_1 S_3 \rangle \approx 0.14$, thus the local spins on dots 1 and 3 are likely to be ferromagnetic due to the RKKY interaction mediated by t. Here, $\langle S_1 S_2 \rangle$ and $\langle S_1 S_3 \rangle$ could not reach the ideal value of spin singlet and triplet respectively, for the ground state here is also frustrated, and the many-body states of $(n_1 n_2 n_3)$ may include configurations such as $(\uparrow\downarrow\, 0)$ (or $(0\, \downarrow\uparrow)$), $(\uparrow\, 0\, \uparrow)$ and $(\uparrow\downarrow\uparrow)$. As t increases to about $t_c \approx 0.0102$, one finds an abrupt change in $\langle n_i \rangle$ and $\langle S_i S_j \rangle$, indicating a first order QPT, e.g., $\langle n_1 \rangle$ drops to 0.42, and $\langle S_1 S_3 \rangle$ drops to -0.1. When t is large enough, e.g., $t = 0.2$, $\langle n_1 \rangle \approx 0.5$, $\langle n_2 \rangle \approx 1.0$, $\langle S_1 S_2 \rangle \approx -0.2$, and $\langle S_1 S_3 \rangle \approx -0.1$, thus dot 1 (3) is empty, while dots 3 (1) and 2 are singly occupied with antiparallel spin configuration, similar to the cases above.

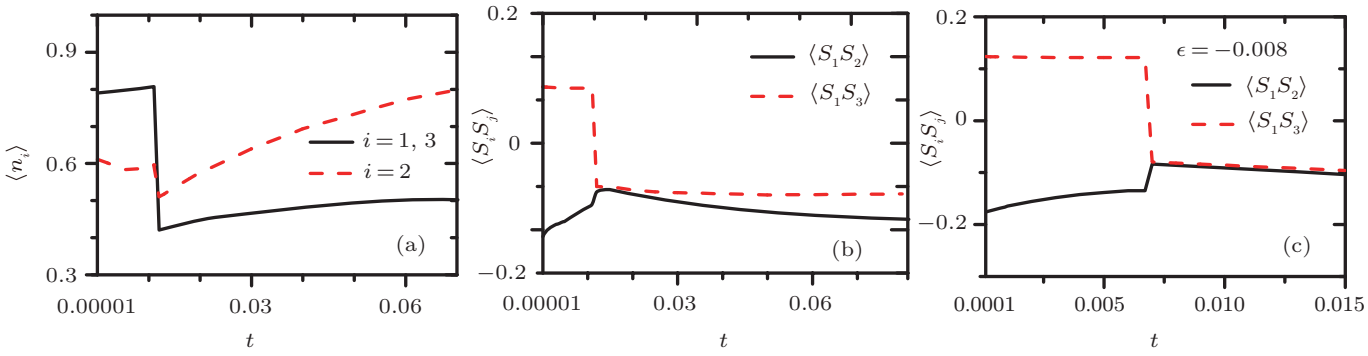


Fig. 5. (color online) (a) and (b) $\langle n_i \rangle$ and $\langle S_i S_j \rangle$ as functions of t when ϵ is set to be $\epsilon = -0.01$. (c) $\langle S_i S_j \rangle$ as a function of t for $\epsilon = -0.008$. The remaining parameters are given the same as Fig. 1.

Figures 6(a) and 6(b) describe $T(\omega)$ for different t. It is seen when t is absent that there is a sharp dip at $\omega = 0$, corresponding to zero conductance (see Fig. 6(c)), which could be attributed to the fact that in this case two singly occupied dots are arranged anti-parallelly, and the present PTQD model maps to a two impurity Anderson model with large inter-dot hopping and the Kondo peak is suppressed.[51] When t is turned on, e.g., $t = 0.011$, the dip is filled up continuously, and the charge transport is enhanced (Figs. 6(a) and 6(c)). In this process, the proportion of configuration $(\uparrow\downarrow\uparrow)$ grows with increasing t, thus dot 1 (3) and dot 2 are more likely to form a spin singlet, and the remaining one contributes to the enhanced conductance. Correspondingly, the electrons on orbital f_a increase to about 1.0. However, in this regime, G could not reach the unitary limit since orbital f_b connected with f_a through a hopping term $\sqrt{2}t/3$, which arises during the canonical transformation above, i.e., Eq. (7). Since orbital f_c is isolated, the present model could be considered as a side-coupled double dot structure, and the conductance decreases with growing inter-dot hopping.[52] When t exceeds the critical point t_c, a broadened peak develops at the left side of $T(\omega)$, which moves toward the left when t grows continuously. In this process, $\langle n'_b \rangle$ and $\langle n'_c \rangle$ drop to zero, thus the PTQD model maps to a single impurity Anderson model. On the other hand, $\langle n'_a \rangle$ increases from 1.27 to 2.0 gradually, hence G decreases to 0.0 successively according to the Freidel sum rule.[53,54] It is worth noting that it is convenient for the critical point t_c to be evaluated by the level of f_b, i.e., with increasing t, the charge number $\langle n'_b \rangle$ drops from 1.0 to 0.0, the critical point is just the point where the singly-occupied energy level of f_b equals to the empty level, which gives $t_c \approx -3\epsilon/4$. In Fig. 5(c), we also show $\langle S_i S_j \rangle$ as functions of t for fixed $\varepsilon = -0.008$. One finds the behaviors are similar to $\epsilon = -0.01$, thus our above discussions are robust in the regime $N_{\rm tot} \approx 2.0$.

For initial charge number $N_{\rm tot} \approx 4.0$, 5.0, and 6.0, the numerical results are similar to the cases $N_{\rm tot} \approx 2.0$, 1.0, and 0.0 respectively, due to particle-hole symmetry. Therefore, we neglect them in the present work.

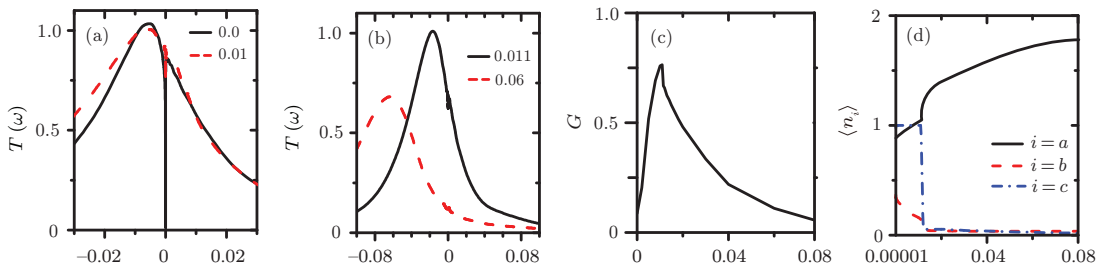


Fig. 6. (color online) (a) and (b) $T(\omega)$ at zero temperature in terms of different t. (c) and (d) G and $\langle n_i' \rangle$ as functions of t for $\epsilon = -0.01$. The remaining parameters are given the same as Fig. 5.

4. Conclusion

In conclusion, we have studied the quantum phase transition and charge transport for a parallel triple dot device in the strongly correlated limit. We focus our attention on the effect of inter-dot hopping t beyond the Kondo regime, and we find the quantum behaviors depend closely on the initial electron number on the dots, which could be adjusted by the dot level through external gate voltage. For instance, when the initial charge number of the dots $N_{\rm tot} \approx 0.0$, it grows continuously with increasing t. When t is large enough, dot 1 (3) and dot 2 form a spin singlet, while dot 3 (1) is empty. The linear conductance G reveals a peak shape and reaches to almost its unitary limit at the point $t = 3\epsilon/4$, where the bonding orbital is singly occupied and an orbital spin-1/2 Kondo effect could be found between the conduction leads and the bonding orbital. In the regime $N_{\rm tot} \approx 1.0$, G could be considered as a part of the above case and the quantum state is similar to the case $N_{\rm tot} \approx 0.0$ as t is large enough. When the initial charge number $N_{\rm tot} \approx 2.0$, we find the ground state is a magnetic-frustration phase and G is nearly zero when t is absent. This phase is sensitive to t, and is replaced by another mixture state even though t is just 0.1×10^4. G increases due to the charge number of the bonding orbital grows to 1.0. When t increases to $t_c \approx -3\epsilon/4$, a first order QPT could be found, and a large peak develops in the transmission coefficient $T(\omega)$. As t is large enough, one of dots 1 and 3 forms a spin singlet with dot 2, while the remaining one is empty, similar to $N_{\rm tot} \approx 1.0$ and 0.0 with large t.

Our results could be used to describe the strongly correlated effects for triple level semiconductor or unimolecular electronic devices connected to the conduction band. We firmly believe that our work not only settled the underlying physical mechanism for the charge transport and phase transition for a PTQD system affected by the inter-dot hopping beyond the Kondo regime, but it may also provide appropriate guidelines for related experiments.

References

[1] Loss D and DiVincenzo D P 1998 *Phys. Rev. A* **57** 120
[2] Tanamoto T 2000 *Phys. Rev. A* **61** 022305
[3] Heersche H B, de Groot Z, Folk J A, Kouwenhoven L P and van der Zant H S J 2006 *Phys. Rev. Lett.* **96** 017205
[4] Zaffalon M, Bid A, Heiblum M, Mahalu D and Umansky V 2008 *Phys. Rev. Lett.* **100** 226601
[5] Fang D K, Wu S Q, Zou C Y and Zhao G P 2012 *Chin. Phys. Lett.* **29** 037303
[6] Büsser C A and Heidrich-Meisner F 2013 *Phys. Rev. Lett.* **111** 246807
[7] Luo K, Wang F Q, Liang R S and Ren Z Z 2014 *Chin. Phys. B* **23** 107103
[8] Wong A, Ngo A T and Ulloa S E 2016 *Phys. Rev. B* **94** 155130
[9] Kleeorin Y and Meir Y 2017 *Phys. Rev. B* **96** 045118
[10] Taylor J M, Srinivasa V and Medford J 2013 *Phys. Rev. Lett.* **111** 050502
[11] Wang B C, Cao G, Li H O, Xiao M, Guo G C, Hu X D, Jiang H W and Guo G P 2017 *Phys. Rev. Appl.* **8** 064035
[12] Friesen M, Ghosh J, Eriksson M A and Coppersmith S N 2017 *Nat. Commun.* **8** 15923
[13] Zhang C X, Yang X C and Wang X 2018 *Phys. Rev. A* **97** 042326
[14] Kim M R and Ma D 2015 *J. Phys. Chem. Lett.* **6** 85
[15] Beltako K, Cavassilas N and Michelini F 2016 *Appl. Phys. Lett.* **109** 073501
[16] Schröer D, Greentree A D, Gaudreau L, Eberl K, Hollenberg L C L, Kotthaus J P and Ludwig S 2007 *Phys. Rev. B* **76** 075306
[17] Stopa M 2002 *Phys. Rev. Lett.* **88** 146802
[18] Vidan A, Westervelt R M, Stopa M, Hanson M and Gossard A C 2004 *Appl. Phys. Lett.* **85** 3602
[19] Žitko R, Bonča J, Ramšak A and Rejec T 2006 *Phys. Rev. B* **73** 153307
[20] Huang R, Ming S W and Wang Y 2012 *Chin. Phys. Lett.* **29** 047201
[21] Baruselli P P, Requist R, Fabrizio M and Tosatti E 2013 *Phys. Rev. Lett.* **111** 047201
[22] López R, Rejec T, Martinek J and Žitko R 2013 *Phys. Rev. B* **87** 035135
[23] Žitko R and Bonča J 2007 *Phys. Rev. Lett.* **98** 047203
[24] Tooski S B, Ramšak A and Bułka B R 2016 *Physica E* **75** 345
[25] Pöltl C, Emary C and Brandes T 2009 *Phys. Rev. B* **80** 115313
[26] Zhu J and Li G 2012 *Phys. Rev. A* **86** 053828
[27] Wang W Z 2007 *Phys. Rev. B* **76** 115114
[28] Mitchell A K, Jarrold T F and Logan D E 2009 *Phys. Rev. B* **79** 085124
[29] Mitchell A K and Logan D E 2010 *Phys. Rev. B* **81** 075126
[30] Xiong Y C, Huang H M, Zhao W L and Laref A 2017 *J. Phys.: Condens. Matter* **29** 405601
[31] Xiong Y C, Zhang J, Zhou W H and Laref A 2017 *Chin. Phys. B* **26** 097102
[32] Jiang Z T, Sun Q F and Wang Y P 2005 *Phys. Rev. B* **72** 045332
[33] Lobos A M and Aligia A A 2006 *Phys. Rev. B* **74** 165417
[34] Ladrón de Guevara M L and Orellana P A 2006 *Phys. Rev. B* **73** 205303
[35] Chiappe G, Anda E V, Ribeiro L C and Louis E 2010 *Phys. Rev. B* **81** 041310(R)
[36] Andrade J A and Cornaglia P S 2016 *Phys. Rev. B* **94** 235112
[37] Wang W Z 2008 *Phys. Rev. B* **78** 235316
[38] Vernek E, Büsser C A, Martins G B, Anda E V, Sandler N and Ulloa S E 2009 *Phys. Rev. B* **80** 035119
[39] Oguri A, Amaha S, Nishikawa Y, Numata T, Shimamoto M, Hewson A C and Taruch S 2011 *Phys. Rev. B* **83** 205304

[40] Xiong Y C, Wang W Z, Luo S J, Yang J T and Huang H M 2016 *J. Magn. Magn. Mater.* **399** 5
[41] Krishna-murthy H R, Wilkins J W and Wilson K G 1980 *Phys. Rev. B* **21** 1003
[42] Krishna-murthy H R, Wilkins J W and Wilson K G 1980 *Phys. Rev. B* **21** 1044
[43] Bulla R, Costi T A and Pruschke T 2008 *Rev. Mod. Phys.* **80** 395
[44] Meir Y, Wingreen N S and Lee P A 1993 *Phys. Rev. Lett.* **70** 2601
[45] Žitko R and Bonča J 2007 *Phys. Rev. B* **76** 241305
[46] Proetto C R and López A 1981 *Phys. Rev. B* **24** 3031
[47] Simonin J 2006 *Phys. Rev. Lett.* **97** 266804
[48] Xiong Y C, Zhao W L and Luo S J 2017 *Superlattice Microst.* **109** 394
[49] Žitko R and Bonča J 2006 *Phys. Rev. B* **74** 045312
[50] Ding G H, Ye F and Dong B 2009 *J. Phys.: Condens. Matter* **21** 455303
[51] Xiong Y C, Luo S J, Huang H M and Yang J T 2015 *J. Supercond. Nov. Magn.* **28** 2553
[52] Cornaglia P S and Grempel D R 2005 *Phys. Rev. B* **71** 075305
[53] Langreth D C 1966 *Phys. Rev.* **150** 516
[54] Ng T K and Lee P A 1988 *Phys. Rev. Lett.* **61** 1768